Asian Journal of Chemistry; Vol. 35, No. 2 (2023), 513-521

ASIAN JOURNAL OF CHEMISTRY

https://doi.org/10.14233/ajchem.2023.26934

Study on Fluorine Removal Performance of Gibbsite by Different Calcined Temperature

XIUWU LIU[1,*], YANG ZHONG[1], YUXING WANG[1], JILIN CAO[1], LEIJIAO GE[2,*], SYED KASHIF ALI[3] and ISLAM MAZAHIRUL[4]

[1]School of Chemical Engineering, Hebei University of Technology, 5340 Xiping Road, Beichen District, Tianjin 300401, P.R. China
[2]School of Electrical Information and Engineering, Tianjin University, Tianjin 300072, P.R. China
[3]Department of Chemistry, Faculty of Science Jazan University, Jazan, PO Box 114, Saudi Arabia
[4]Department of Biology, Faculty of Science, Jazan University, Jizan, Saudi Arabia

*Corresponding authors: Tel: +86 13502198210; E-mail: tjxiuwu@163.com; legendglj99@tju.edu.cn

Received: 16 November 2022; *Accepted*: 25 January 2023; *Published online*: 30 January 2023; AJC-21138

When applied to wastewater treatment, natural gibbsite has a low fluorine capacity and is therefore rarely used. In this work, the gibbsite was calcined at different temperatures to improve the fluoride adsorption capacity. The adsorption responsible parameters, such as calcination temperature and time, initial fluoride concentration, dosage, reaction time and temperature were optimized. The results showed that the adsorption capacity of fluorine ion varies significantly by the gibbsite calcined at different temperatures. The best fluorine removal effect is the gibbsite calcined at 573 K for 0.75 h and its adsorption fluoride capacity of 8.3470 mg/g, which is 7.4 times that of natural gibbsite under the same conditions. Calcination temperature on its structural properties by means of scanning electron microscopy (SEM), thermogravimetric and differential thermal analysis (TGA/DSC), X-ray diffraction (XRD) and Brunauer-Emmett-Teller (BET) for the gibbsite were investigated. The results of characterization analysis showed that the phase composition of gibbsite calcined at different temperatures is different and the significantly different effect of fluorine removal may be attributed to the increase of specific surface area after calcination. The pseudo-second-order kinetic model and Langmuir adsorption isotherm model can better describe the fluorine removal process of gibbsite calcined at high temperature.

Keywords: Trace fluorine wastewater, Fluoride removal, Gibbsite, Calcination temperature.

INTRODUCTION

Pollution of the natural world has become more prominent as the economy has expanded. Most industrial activities, such as metal smelting, metal surface cleaning, pesticides, metallurgy, electronics industry, *etc*. discharged large amounts of fluorine containing wastewater every year. If these fluorine containing wastewater is directly discharged without treatment, it will not only pollute the water resources, but also seriously threaten human health [1]. Therefore, these industrial wastewater with excessive fluoride should be treated to make them meet the requirements of the discharge standards.

At present, the technologies of fluoride removal mainly include adsorption, ion exchange, membrane separation, coagulation sedimentation, electrochemical, *etc.* [2-8]. Due to its simple operation, stable adsorption effect and low cost, the adsorption method is considered to be the most ideal fluoride removal technology. Commonly adsorbents, such as activated carbon, biological adsorbents, natural mineral adsorbents and rare earth oxide adsorbents have been widely used in the treatment of fluoride containing wastewater [9-11].

The defluorination properties of several natural minerals, *e.g*. diaspore, bentonite, zeolite, kaolin had also been reported in the literature [12-14]. Corral-Capulin *et al*. [15] investigated the influence of chemical and thermal treatments on the fluoride removal from water by three minerals. Metallic species interact with minerals by coordination with hydroxyl groups or precipitation on minerals surfaces. Compared with aluminum modified materials for water treatments by precipitation on minerals surfaces, iron-modified materials were the better options for fluoride removal from aqueous solutions by coordination with hydroxyl groups. Onyango *et al.* [16] investigated the effect of Al^{3+} and La^{3+} modified Na^{+} combined zeolite on fluoride removal. Aluminum exchanged zeolite was more effective than lanthanum-exchanged zeolite. Nagaraj *et al.* [17] prepared mineral (Al^{3+}, La^{3+}, Ce^{3+})-substituted hydroxyapatite (mHAp)

composite for the fluoride removal from drinking water and the best fluoride removal efficiency of mHAp adsorbent reached 93%.

In previous study [18], the results of fluoride removal were satisfactory and the concentration of fluorine ion is reduced from 30 mg/L to 3.08 mg/L using La^{3+}-modified gibbsite, but the adsorption capacityof natural and modified gibbsite towards fluorine is not satisfactory. In this experiment, the effects on fluoride adsorption capacity of gibbsite calcined at different temperature were investigated. The influence factors, such as calcination temperature, calcination time, initial fluoride ion concentration and dosage of adsorbent, reaction time and temperature were also optimized.

EXPERIMENTAL

The natural gibbsite was provided by a mineral company in Yunnan Province, P.R. China. In this work, the details of the chemicals used, supplier information, purities and CAS numbers are given in Table-1.

Characterization: In this study, a German X-ray diffractometer (XRD) manufactured by Bruker AXS Co., Ltd., model Da Vinci, was utilized. The test conditions were operating voltage 40 kW, operating current 200 mA, Cu target, diffraction angle 2θ =10-80º at the scanning speed of 12º/min. Thermogravimetric analysis and differential scanning calorimetry (TGA/DSC) (SDT Q-600, TA Instruments-water LLC, heating rate 20 min^{-1} in flow air); field emission scanning electron microscopy (SEM) (Ametekoctane Plus, operated at 10 kV). Nitrogen adsorption–desorption measurements for the adsorbents were performed using a Micromeritics ASAP 2020M+C instrument and Barrett-Emmett-Teller (BET) was used to calculate the specific surface area, the a_s method was used to calculate the corresponding pore volumeand the external surface area of adsorbent, *etc*.

Batch defluoridation experiments: The factors affecting the fluorine removal efficiency of gibbsite, which was calcined at different temperatures, were investigated. Fluoride removal experiments were carried out at different calcination temperature, calcination time, initial fluoride ion concentration, the dosage, reaction time and temperature to explore the influence of various factors on the performance of fluoride removal.The experimental results of fluoride removal were analyzed by the fluorine removal rate R(%), the adsorption of the fluoride ion capacity q_e (mg/g) at equilibrium and the adsorption of fluoride ion capacity q_t (mg/g) at time t. The parameters *viz*. R(%), q_e (mg/g), q_t (mg/g) were calculated by the following equation: where C, C_t and C_e are the initial state, time t and equilibrium fluoride ion concentration (mg/L), respectively; V is the volume (L) of fluoride ion solution, and M is the mass of gibbsite.

$$R\ (\%) = \frac{C - C_t}{C} \times 100 \quad (1)$$

$$q_e = (C - C_e) \times \frac{V}{M} \quad (2)$$

$$q_t = (C - C_t) \times \frac{V}{M} \quad (3)$$

RESULTS AND DISCUSSION

Effect of calcination temperature on fluoride removal: In order to explore the effect of calcination temperature on the performance of fluoride removal, 3 g/L of natural gibbsite or gibbsite calcined at different temperatures *viz*. 523, 548, 573, 598, 623, 723, 823, 923 and 1023 K were added at the initial concentration of 30 mg/L fluoride ion solution at room temperature to carry out the fluoride removal experiment and agitated for 120 min. The fluorine removal rate of natural gibbsite was 11.23% and its the adsorption capacity was found to be 1.1230 mg/g (Fig. 1). As the calcination temperature increased from 523 K to 1023 K, the fluoride removal rate increased from 49.07% to 78.02% at first and then decreased to 70.12%, whereas the adsorption capacity increased from 4.9067 to 7.8017 mg/g and then decreased to 7.0117 mg/g. Therefore, the optimal calcination temperature for fluoride removal by gibbsite calcined was 573 K.

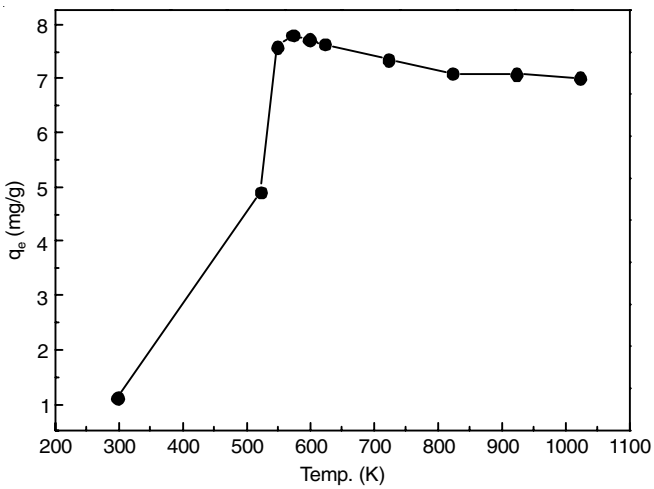

Fig. 1. Effect ofcalcination temperature on fluoride removal

Effect of calcination time: In order to explore the influence of calcination time on the performance of fluoride removal, 3 g/L of gibbsite calcinated at 573 K for 0.5, 0.75, 1, 1.5, 2 and 2.5 h was added to the initial concentration of 30 mg/L fluoride

TABLE-1
CHEMICAL NAMES, SUPPLIER INFORMATION, PURITIES AND CAS NUMBERS FOR ALL CHEMICALS USED

Chemical name	m.f.	m.w.	Supplier	Purity (%)	CAS number
Sodium fluoride	NaF	41.99	Fuchen	98.0	7681-49-4
Sodium hydroxide	NaOH	40.00	Fuchen	96.0	1310-73-2
Sodium chloride	NaCl	58.44	Hengshan	AR	7647-14-5
Trisodium citrate	$C_6H_5Na_3O_7 \cdot 2H_2O$	294.10	Hengshan	99.0	6132-04-3
Glacial acetic acid	CH_3COOH	60.05	Fuchen	99.5	64-19-7

ion solution at room temperature and the experiment data was recorded until the adsorption reached approximately equilibrium. As the calcination time increased from 0.5 h to 2.5 h, the adsorption capacity increased from 7.9257 to 8.3470 mg/g and then decreased to 7.3880 mg/g, whereas the fluorine removal rate increased from 79.26% to 83.47% and then decreased to 73.88% (Fig. 2). Therefore, the optimal calcination time of gibbsite was 0.75 h.

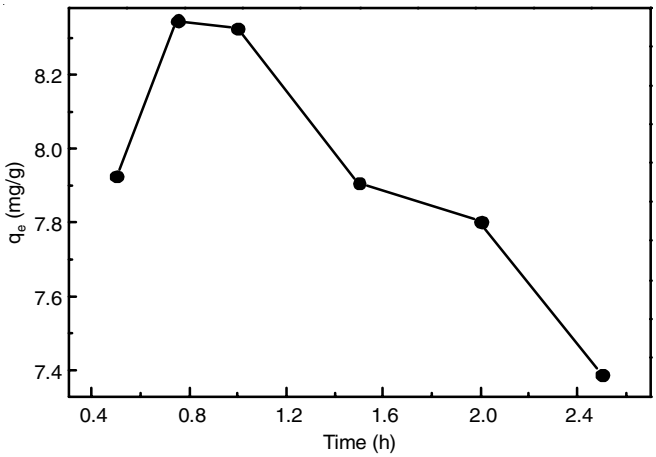

Fig. 2. Effect of calcination time on fluoride removal

Effect of adsorbent dosage: In order to investigate the effect of dosage of calcined gibbsite on the performance of fluoride removal, 1, 2, 3, 4, 5, 6, 7, 8, 9 and 10 g/L of calcined gibbsite at 573 K for 0.75 h were added to the initial concentration of 30 mg/L fluoride ion solution at room temperature and the experiment data was recorded until the adsorption reached approximately equilibrium. When the amount of calcined gibbsite was 1 g/L, the fluorine removal rate was 41.09% and its adsorption capacity was 12.327 mg/g. With increasing dosage of calcined gibbsite, the fluorine removal rate increased significantly. When 9 g/L calcined gibbsite was added, the fluoride removal rate reached 93.85% and its adsorption capacity was 3.1282 mg/g (Fig. 3). The residual fluoride ion concentration in the solution was 1.84 mg/L. Compared with previous experimental results that the concentration of fluorine ion was reduced from 30 mg/L to 3.08 mg/L by adding 40 g/L La^{3+}-modified gibbsite [18], the fluorine removal effect of calcined gibbsite was better. When the dosage increased to 10 g/L, the fluoride removal rate was 93.97% and only increased 0.13% than that of 9 g/L dosage. Therefore, the optimal dosage of calcined gibbsite was 9 g/L.

Effect of initial fluoride concentration: In order to investigate the effect of initial fluoride ion concentration on fluoride removal performance, 9 g/L of gibbsite calcined at 573 K for 0.75 h was added to the initial concentration of 10, 20, 30, 40, 50, 70, 100 mg/L fluoride ion solution at room temperature and the experiment data was recorded until the adsorption reached approximately equilibrium. When the initial fluoride concentration was 10 mg/L, the fluoride removal rate was 95.63% and the fluorine removal rate gradually decreased as the initial fluoride ion concentration increased (Fig. 4). When the initial fluoride ion concentration reached 100 mg/L, the fluoride

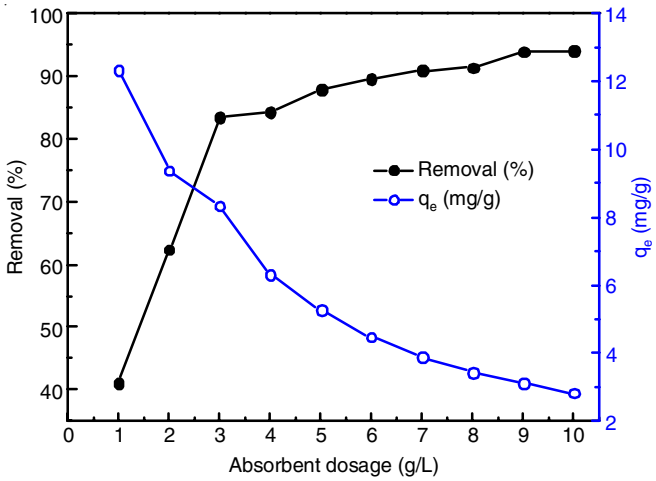

Fig. 3. Effect of adsorbent dosage on fluoride removal

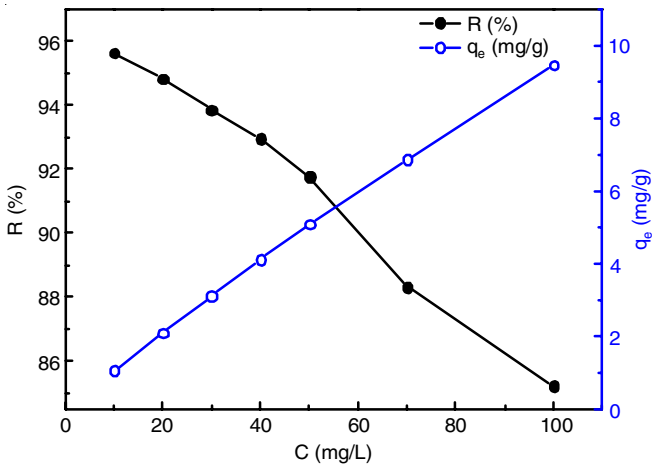

Fig. 4. Effect of initial fluoride concentration on fluoride removal

removal rate decreased to 85.23%. As the initial fluoride ion concentration increased, the adsorption capacity increased significantly from 1.0625 mg/g to 9.4700 mg/g.

Effect of reaction time: Gibbsite (9 g/L) calcined at 573 K for 0.75 h was added to the initial fluoride concentration of 10 and 30 mg/L at room temperature. The first 20 min was the rapid fluorine removal process.The adsorption capacity and the fluorine removal rate of calcined gibbsite reached 0.9629 mg/g and 89.99% respectively in 10 mg/L initial fluoride concentration solution and that reached 2.7948 mg/g and 89.12%, respectively in 30 mg/L initial fluoride concentration solution (Fig. 5). As the adsorption time continued to prolong, the fluorine removal rate slowly increased. When the reaction reached 120 min, the fluorine removal rate separately reached 95.63% and 93.85% in 10 and 30 mg/L initial fluoride concentration solution and their corresponding adsorption capacities were 1.0625 mg/g and 3.1282 mg/g, respectively. Compared with calcined gibbsite, the adsorption capacitiesof natural gibbsite were 0.2020 mg/g and 0.5182 mg/g under the same reaction condition in previous study. As observed from Fig. 5, when the adsorption time is 120 min, the adsorption capacities remained unchanged and the adsorption basically reached equilibrium in 10 and 30 mg/L initial fluoride concentration solution, hence the optimal reaction time determined was 120 min.

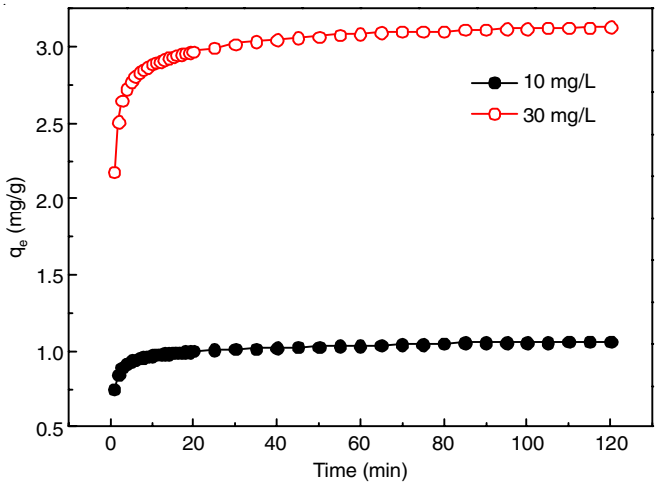

Fig. 5. Effect of reaction time on fluoride removal

Effect of reaction temperature: Optimizing the above mentioned parameters, the effect of reaction temperature on the performance of fluorine removal was also investigated. With the increase of the reaction temperature, the adsorption capacity reduced from 3.1282 mg/g to 2.9250 mg/g and the fluorine removal rate decreased from 93.85% to 87.75% (Fig. 6). As a result, the optimal fluorine removal temperature is 298 K (room temperature).

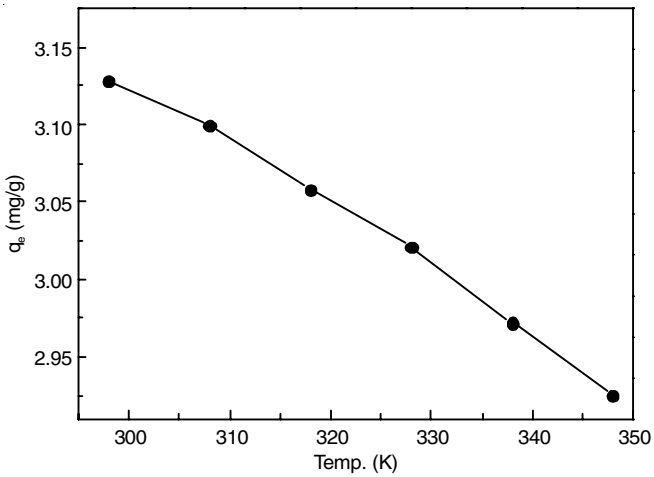

Fig. 6. Effect ofreaction temperature on fluoride removal

Effect of Co-coexisting anions: If wastewater contains other coexisting ions, the fluoride removal efficiency may be greatly influenced. The effects of the coexisting ions, such as Ca^{2+}, Mg^{2+}, NO_3^-, SO_4^{2-}, Cl^- and HCO_3^- were studied. Calcined gibbsite were added to the solution containing 30 mg/L F^- ion and 60 mg/L coexisting ion. The influences of different coexisting ions on the fluoride adsorption capacity of calcined gibbsite are different. Comparing with co-ions, Mg^{2+} and Ca^{2+} ions slightly enhanced the F^- adsorption, while NO_3^- and Cl^- ions negligible hindered the F^- adsorption. However, SO_4^{2-} and HCO_3^- ions have strong restriction effects on the F^- adsorption. Corresponding to in the presence of SO_4^{2-} and HCO_3^- ions, the fluoride adsorption capacity of calcined gibbsite decreased to 77.3% and 63.8%, respectively (Fig. 7). As a result, the fluoride removal experiment couldn't be accomplished until the coexisting SO_4^{2-} and HCO_3^- ions were eliminated.

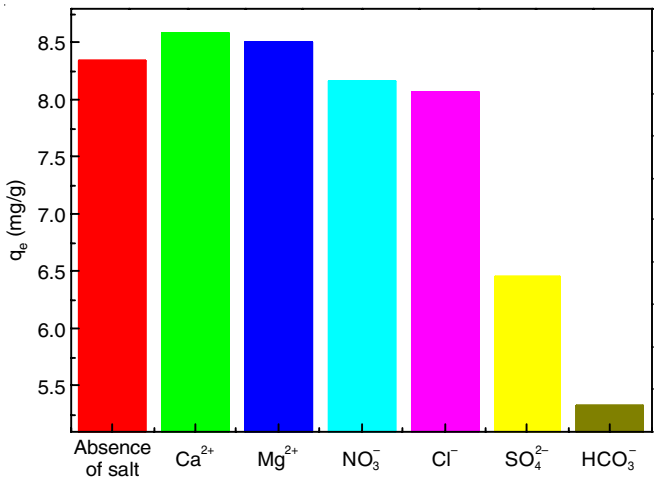

Fig. 7. Effect of Co-coexisting anions on fluoride removal

Morphological studies: The scanning electron microscope (SEM) results of gibbsite uncalcined and calcined at 573 K for 0.75 h are shown in Fig. 8. It can be seen that gibbsite was in block and flaky irregular shape with void structure, which can be used as an adsorbent. The calcined gibbsite particles appeared agglomerated with each other and the surface was loose. Due to extensive dehydration, which resulted in the formation of cracks, fine grains and larger gaps between the grains, the adsorption performance was improved.

TGA/DSC analysis: DSC curve (Fig. 9) showed a weak endothermic peak from room temperature to 70 ºC, which was in agreement with the loss of mass (1.25 wt.%) in the TGA curve. This was due to the evaporation of water adsorbed on the surface of gibbsite. The next endothermic peak in DSC curve at 250-380 ºC corresponds to the loss of mass (14.37%). This was mainly due to the partial $Al(OH)_3$ decomposition and the corresponding chemical reaction equations are $Al(OH)_3/AlOOH + H_2O$ and $AlOOH \rightarrow \chi\text{-}Al_2O_3 + H_2O$. The weight of the sample decrease since some of the water evaporated. The third relatively weak endothermic peak in DSC curve at 400-570 ºC correspond to the loss of mass (3.35%) in TGA curve, which is due to the partial AlOOH decomposition and the corresponding reaction equation was $AlOOH \rightarrow \gamma\text{-}Al_2O_3 + H_2O$. After that a steady drop of the thermogravimetric curve was mostly caused by the decomposition reaction of sample.

XRD studies: The gibbsite calcined at different temperatures were characterized by XRD and the results are shown in Fig. 10, whereas the XRD images of gibbsite calcined for 0.75 h and 2 h (time) are shown in Fig. 10a. From Fig. 10a, the characteristic peaks of gibbsite calcined at 523 K are basically consistent with that of uncalcined gibbsite. The d-values of diffraction peaks at 4.8633, 4.3879, 4.3350, 3.3666, 2.4687, 2.4565 and 2.3897 nm; corresponding to 2θ 18.227º, 20.221º, 20.470º, 26.453º, 36.362º, 36.549º and 37.609º are the $Al(OH)_3$ characteristic peaks. When the gibbsite calcined at 573 K and 623 K, the characteristic diffraction peaks at 14.457º, 28.197º, 38.490º appeared, which corresponded to

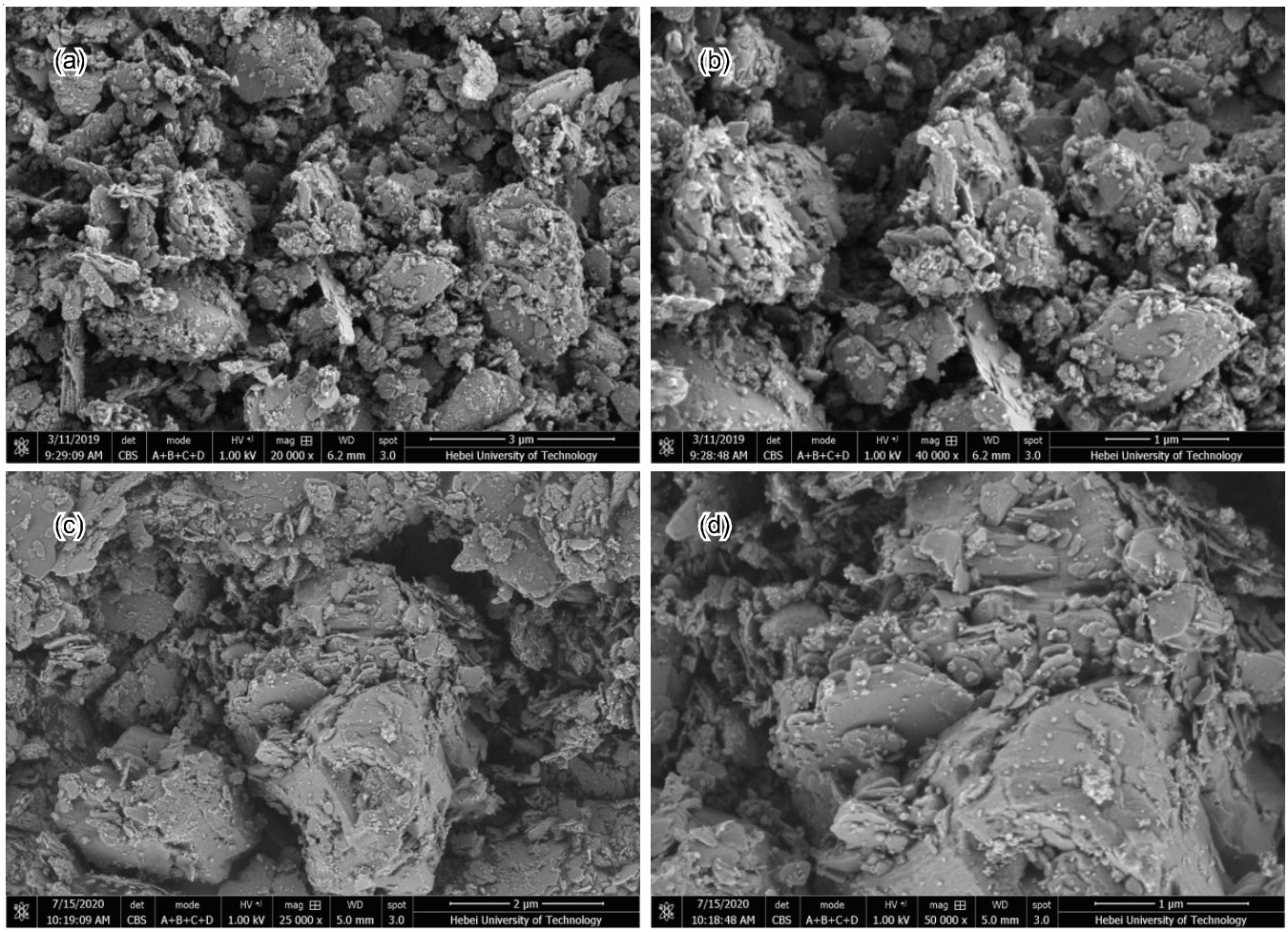

Fig. 8. SEM image of natural gibbsite and calcined gibbsite at 573 K for 0.75 h (a and b - natural gibbsite; c and d - calcined gibbsite)

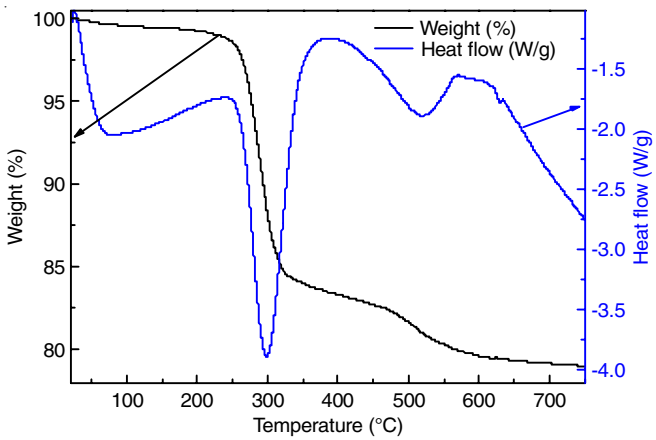

Fig. 9. Curves of thermogravimetric and differential thermal analysis of gibbsite

AlOOH characteristic peaks. At the same time, the χ-Al_2O_3 characteristic diffraction peak at 41.182º also appeared and the characteristic diffraction peak of $Al(OH)_3$ become weakened, which is consistent with the description of the TGA-DSC curve. When gibbsite calcined at 723-1023 K, the characteristic diffraction peaks of $Al(OH)_3$ disappeared, while the characteristic diffraction peaks of γ-Al_2O_3 at 2θ of 38.451º, 42.582º and 67.019º appeared. The XRD images of gibbsite calcined at 573 K for 0.75 h (the optimal fluorine removal effect) and that calcined at 573 K for 2 h are shown in Fig. 10b. As the calcination time increased, the highest characteristic peak of $Al(OH)_3$ disappeared and the residual amount of $Al(OH)_3$ dropped sharply. Therefore, the dehydroxylation of gibbsite had significant effect on the material surface area and eventually leaded to the effect of fluoride removal.

BET surface studies: The nitrogen adsorption-desorption isotherms of natural gibbsite and calcined gibbsite at 573 K for 0.75 h are shown in Fig. 11 and their corresponding pore structure parameters are shown in Table-2. It can be seen that the adsorption-desorption isotherms of natural and calcined gibbsite were of type IV isotherm. After calcination, the specific surface area of gibbsite greatly increased from 29.4808 to 224.4474 m^2/g and the corresponding pore volume increased from 0.03612 to 0.1309 cm^3/g. The average pore size of gibbsite decreases from 9.9693 nm to 3.9447 nm and the shrinkage of pore may be due to the decomposition of aluminum hydroxide. As a result of its dramatically increased specific surface area, calcined gibbsite is capable of providing more adsorption sites and a more effective means of removing fluoride from water. Compared with before and after calcination of gibbsite, the change of fluoride adsorption capacity is basically consistent with that of specific surface area. Therefore, the significant

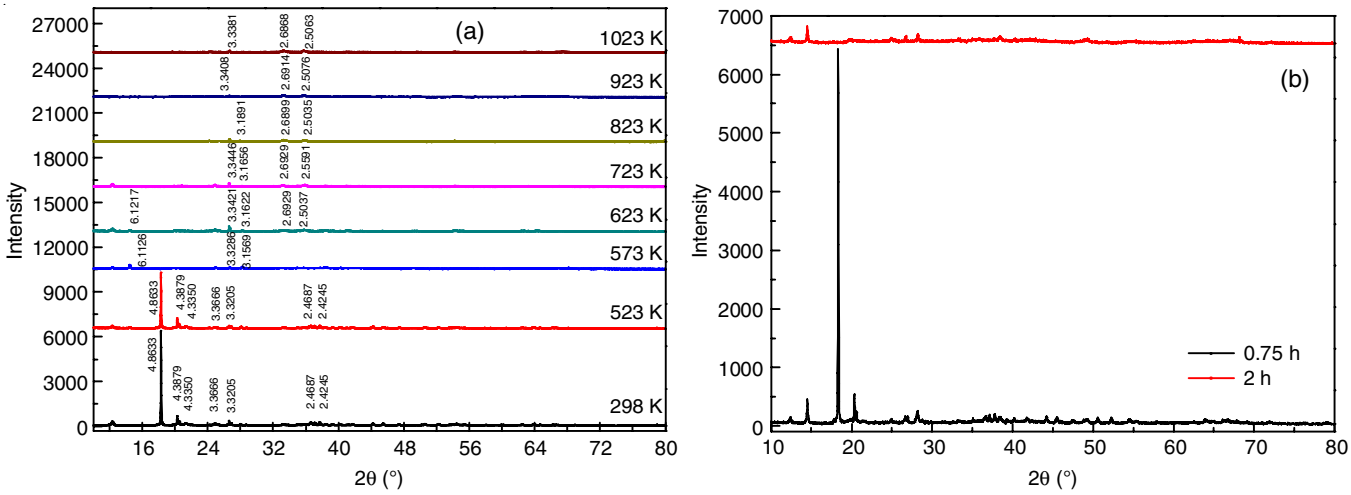

Fig. 10. XRD patterns of gibbsite calcined at different temperature (a) or different time (b)

TABLE-2
TEXTURAL PARAMETERS OF GIBBSITE AND CALCINED GIBBSITE AT 573 K FOR 0.75 h

Sample	Specific surface area (m^2/g)	Average pore size (nm)	Total pore volume (cm^3/g)	Micropore volume (cm^3/g)
Gibbsite	29.4808	9.9693	0.03612	0.006010
Calcined gibbsite at 573 K	224.4474	3.9447	0.13090	0.024200

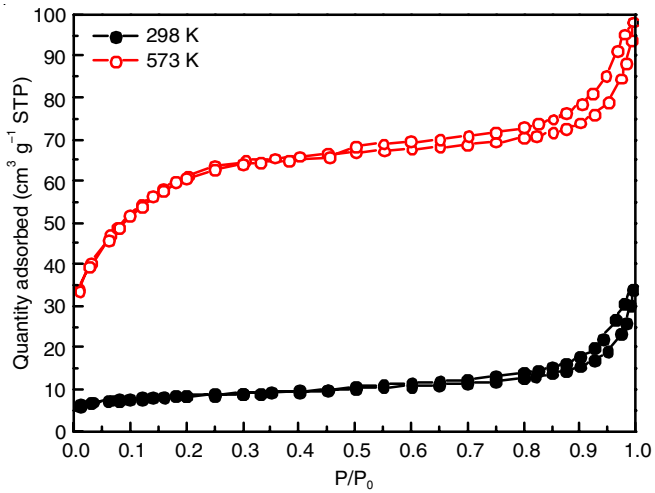

Fig. 11. 77 K Nitrogen adsorption–desorptionisotherms of naturalgibbsite and calcined gibbsite at 573 K for 0.75 h

improvement of fluoride removal efficiency of calcined gibbsite may be attributed to the increase of specific surface area after calcination.

After gibbsite calcined at 573 K for 0.75 h, the phase compositions were AlOOH, χ-Al_2O_3, $Al(OH)_3$ by XRD analysis and TGA/DSC analysis also was consistent with this result. Calcined gibbsite particles appeared to be agglomerated with each other and their surfaces become loosen as evidenced from the SEM images. The specific surface area and pore volume of gibbsite after calcination sharply increased by BET analysis. Due to the changes in the phase composition after calcination, the atomic space structure and surface properties of gibbsite is different, which results in the adsorption performance and ion exchange capacity of F^-. Aluminum oxyhydroxide can have good adsorption performance by transitional alumina in some studies, which was consistent with the present experimental result [19].

Adsorption kinetics: Adsorption kinetics experiments were carried out with 10, 30, 50 mg/L fluoride ion solution and 8, 9, 10 g/L gibbsite calcined at 573 K for 0.75 h, the adsorption kinetics process was described and analyzed by pseudo-first-order model and pseudo-second-order model.

The linear form of pseudo-first-order kinetics and pseudo-second-order kinetics are represented by the following eqns. 4 and 5:

$$\frac{1}{q_t} = \frac{k_1}{q_e t} + \frac{1}{q_e} \quad (4)$$

$$\frac{t}{q_t} = \frac{1}{k_2 q_e^2} + \frac{1}{q_e} t \quad (5)$$

where k_1, k_2 are the separation rate constant of pseudo-first-order adsorption and pseudo-second-order adsorption, respectively. The q_e and k_1 respectively were obtained from the slope and intercept of the linear plot of $1/q_t$ to 1/t, while the q_e and k_2 respectively were obtained from the slope and intercept of the linear plot of t/q_t to t (Fig. 12).

As observed from Table-3, the pseudo-second-order model linear fit of calcined gibbsite is better. The correlation coefficient R^2 has a mean value of 0.99, hence the pseudo-second-order kinetic model can better describe the fluorine removal process of calcined gibbsite.

Adsorption isotherms: The fluorine removal isotherm of calcined gibbsite were conducted at 298, 308 and 318 K by performing adsorption isotherm experiments with the initial concentrations of 10, 20, 30, 40, and 50 mg/L fluoride ion solution. Two models, the Langmuir and the Freundlich adsorption isotherms, were used to define and study the adsorption isotherm process.

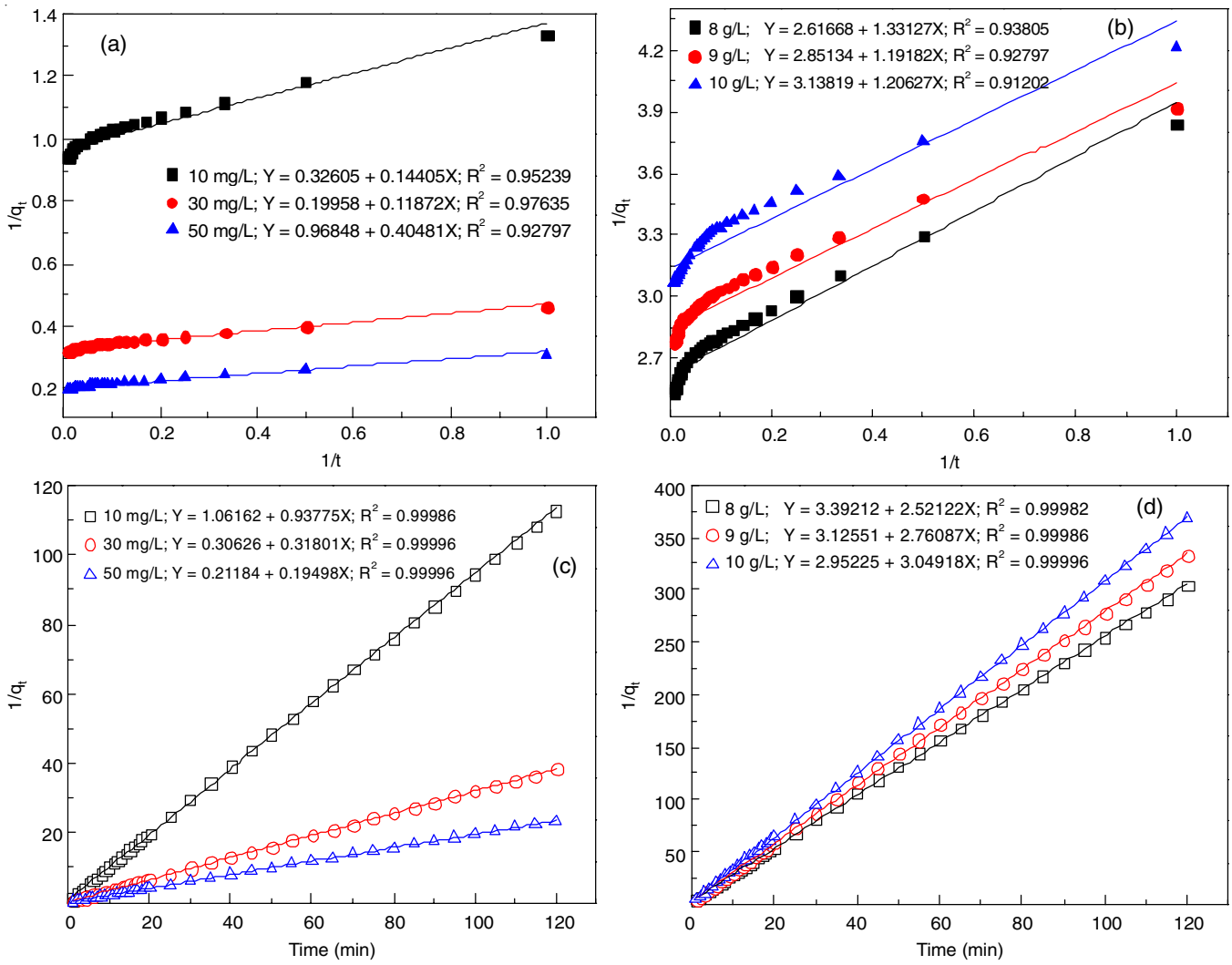

Fig. 12. Pseudo-first-order model (a,b) and Pseudo-second-order model (c,d) of different initial fluoride concentration and adsorbent dosage on calcined gibbsite [a,c - different initial fluoride concentration; b,d- different adsorbent dosage]

TABLE-3
PARAMETERS OF PSEUDO-FIRST-ORDER AND PSEUDO-SECOND-ORDER KINETICS MODEL

C_F- (mg/L)	Gibbsite (g/L)	Pseudo-first-order model			Pseudo-second-order model		
		q_e	k_1	R^2	q_e	k_2	R^2
10	9	3.0670	0.4418	0.95239	1.0664	0.8283	0.99986
30	9	5.0105	0.5948	0.97635	3.1446	0.3302	0.99996
50	9	1.0325	0.4180	0.92797	5.1287	0.1795	0.99996
30	8	0.3822	0.5088	0.93805	0.3966	1.8739	0.99982
30	9	0.3507	0.4180	0.92797	0.3622	2.4388	0.99986
30	10	0.3186	0.3844	0.91202	0.3280	3.1493	0.99996

The linearized Langmuir isotherm and the Freundlich isotherm models are represented by using eqns. 6 and 7:

$$\frac{1}{q_e} = \frac{1}{q_m} + \frac{1}{q_m b C_e} \quad (6)$$

$$\log q_e = \log K_f + \frac{1}{n} \log C_e \quad (7)$$

where C_e and q_e are respectively the equilibrium concentration (mg/L) and equilibrium adsorption capacity (mg/g). B and q_m are Langmuir adsorption constants and saturation adsorption capacity (mg/g). The values of b and q_m were obtained from the slope and intercept of the linear plot of $1/q_e$ to $1/C_e$. n and K_f are empirical constants of Freundlich isotherm model. The n and K_f respectively are obtained from the slope and intercept of the linear plot of log q_e to log C_e (Fig. 13). Since, the linear fit of the Langmuir adsorption isotherm model was better than the Freundlich model as can be deduced from the values of the isotherm parameters given in Table-4.

Adsorption thermodynamics: The thermodynamic parameters for the adsorption process including Gibbs free energy change (ΔG°), enthalpy change (ΔH°), entropy change (ΔS°) can be calculated by the following eqns. 8-11:

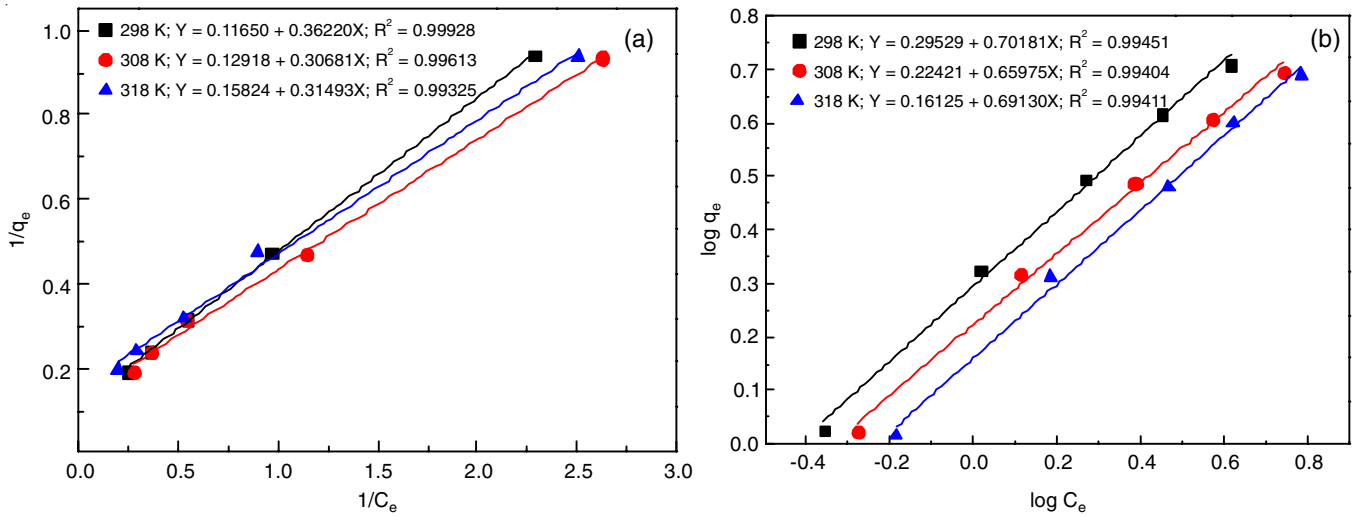

Fig. 13. Curves of Langmuir adsorption isotherm (a) and Freundlich adsorption isotherm (b)

TABLE-4
PARAMETERS OF LANGMUIR ADSORPTION ISOTHERM MODEL AND FREUNDLICH ADSORPTION ISOTHERM MODEL

Temp. (K)	Langmuir			Freundlich		
	q_m	b	R^2	K_f	n	R^2
298	8.5837	0.3216	0.99928	1.9737	1.4249	0.99451
308	7.2711	0.3202	0.99857	1.6758	1.5157	0.99404
318	7.9246	0.2308	0.99823	1.4496	1.4465	0.99411

$$K_0 = \frac{q_e}{C_e} \quad (8)$$

$$\Delta G° = -RT \ln K_0 \quad (9)$$

$$\Delta G° = \Delta H° - T\Delta S° \quad (10)$$

$$\ln K_0 = -\frac{\Delta H°}{RT} + \frac{\Delta S°}{R} \quad (11)$$

where K_o is the adsorption equilibrium constant; q_e is the adsorption capacity of fluoride ion at equilibrium (mg/g); C_e is the fluoride ion concentration at equilibrium (mg/L); R is the gas constant (8.314 J mol^{-1} K^{-1}); T is the absolute temperature (K). The values of ΔHº and ΔSº can be determined by the slope and intercept of the linear plot of ln K_0 *versus* 1/T.

From Table-5, the ΔGº at different temperatures was negative indicated that the spontaneous F^- adsorption process of gibbsite. Thus, at lower temperature, the degree of spontaneity will be greater. Adsorption is an exothermic reaction, as shown by the enthalpy change ($\Delta H° < 0$), which is in agreement with the results of the Langmuir adsorption isotherm studies. When the temperature of the reaction is increased, the fluoride removal process becomes less effective.

TABLE-5
ABSORPTION THERMODYNAMIC DATA OF HIGH TEMPERATURE CALCINED GIBBSITE

Temp. (K)	ΔG° (KJ mol^{-1})	ΔH° (KJ mol^{-1})	ΔS° (J mol^{-1} K^{-1})
298	-5.06		
308	-2.31	-16.44	-46.18
318	-1.70		

Mechanism of fluorine removal of calcined gibbsite: After calcination, the defluoridation ability of gibbsite was greatly improved. Compared with before and after calcination of gibbsite, the surfaces of calcined gibbsite became loose, cracks and fine grains, which promoted the greatly increasing specific surface area and enhanced the F^- adsorption capacity. On the other hand, the radii and charges of F^- and OH^- are similar, so F^- will exchange the hydroxyl groups in the AlOOH of calcined gibbsite obtained by decomposition in the removing fluoride process. Therefore, F^- may be transformed into AlF^{2+}, AlF_3, AlF_4^-, AlF_5^{2-}, *etc.* and finally achieves the purpose of fluorine removal.

Conclusion

In this work, the fluorine removal efficiency rate of gibbsite after calcination is greatly improved. The fluorine removal rate of gibbsite calcined at 573 K for 0.75 h can reach 93.85% and the concentration of fluoride ion in the solution is reduced from 30 mg/L to 1.84 mg/L. Compared with before and after calcination of gibbsite, the change of fluoride adsorption capacity is basically consistent with that of specific surface area. Therefore, the significant improvement of fluoride removal efficiency of calcined gibbsite may be attributed to the increase of specific surface area after calcination. The fluorine elimination process of calcined gibbsite was clearly explained by the pseudo-second-order kinetic and the Langmuir adsorption isotherm models.

ACKNOWLEDGEMENTS

This work was supported by Science and Technology Research Project of Hebei Educational Committee (grant No.

ZD2019042) and Tianjin Natural Science Foundation Special funds of Tianjin Science and Technology Committee (grant No. 17JCTPJC55700).

CONFLICT OF INTEREST

The authors declare that there is no conflict of interests regarding the publication of this article.

REFERENCES

1. N. Akhtar, M.I.S. Ishak, S.A. Bhawani and K. Umar, *Water*, **13**, 2660 (2021); https://doi.org/10.3390/w13192660
2. J. Singh, P. Singh and A. Singh, *Arab. J. Chem.*, **9**, 815 (2016); https://doi.org/10.1016/j.arabjc.2014.06.005
2. M. Mohapatra, S. Anand, B.K. Mishra, D.E. Giles and P. Singh, *J. Environ. Manage.*, **91**, 67 (2009); https://doi.org/10.1016/j.jenvman.2009.08.015
3. H. Liu, W. Jiang, D. Wan and J. Qu, *J. Hazard. Mater.*, **169**, 23 (2009); https://doi.org/10.1016/j.jhazmat.2009.03.053
4. P. Loganathan, S. Vigneswaran, J. Kandasamy and R. Naidu, *J. Hazard. Mater.*, **248-249**, 1 (2013); https://doi.org/10.1016/j.jhazmat.2012.12.043
6. A. Bhatnagar, E. Kumar and M. Sillanpää, *Chem. Eng. J.*, **171**, 811 (2011); https://doi.org/10.1016/j.cej.2011.05.028
7. J. Du, D.A. Sabatini and E.C. Butler, *Chemosphere*, **101**, 21 (2014); https://doi.org/10.1016/j.chemosphere.2013.12.027
8. M.A. Sandoval, R. Fuentes, J.L. Nava and I. Rodriguez, *Sep. Purif. Technol.*, **134**, 163 (2014); https://doi.org/10.1016/j.seppur.2014.07.034
9. E. Kumar, A. Bhatnagar, U. Kumar and M. Sillanpaa, *J. Hazard. Mater.*, **186**, 1042 (2011); https://doi.org/10.1016/j.jhazmat.2010.11.102
10. M.N. Sepehr, V. Sivasankar, M. Zarrabi and M. Senthil Kumar, *Chem. Eng. J.*, **228**, 192 (2013); https://doi.org/10.1016/j.cej.2013.04.089
11. Y. Yu, L. Yu and J. Paul Chen, *Chem. Eng. J.*, **262**, 839 (2015); https://doi.org/10.1016/j.cej.2014.09.006
12. S.P. Kamble, P. Dixit, S.S. Rayalu and N.K. Labhsetwar, *Desalination*, **249**, 687 (2009); https://doi.org/10.1016/j.desal.2009.01.031
13. Y.B. Sun, Q.H. Fang, J.P. Dong, X. Cheng and J. Xu, *Desalination*, **277**, 121 (2011); https://doi.org/10.1016/j.desal.2011.04.013
14. Z.J. Zhang, Y. Tan and M.F. Zhong, *Desalination*, **276**, 246 (2011); https://doi.org/10.1016/j.desal.2011.03.057
15. N.G. Corral-Capulin, A.R. Vilchis-Nestor, E. Gutiérrez-Segura and M. Solache-Rios, *J. Fluor. Chem.*, **213**, 42 (2018); https://doi.org/10.1016/j.jfluchem.2018.07.002
16. M.S. Onyango, Y. Kojima, O. Aoyi, E.C. Bernardo and H. Matsuda, *J. Colloid Interface Sci.*, **279**, 341 (2004); https://doi.org/10.1016/j.jcis.2004.06.038
17. A. Nagaraj, M.A. Munusamy, M. Ahmed, S. Suresh Kumar and M. Rajan, *New J. Chem.*, **42**, 12711 (2018); https://doi.org/10.1039/C8NJ02401D
18. X.W. Liu, Y.X. Wang, X.Y. Cui, S.J. Zhu and J.L. Cao, *J. Chem. Eng. Data*, **66**, 658 (2021); https://doi.org/10.1021/acs.jced.0c00815
19. W.X. Gong, J.H. Qu, R.P. Liu and H.C. Lan, *Chem. Eng. J.*, **189-190**, 126 (2012); https://doi.org/10.1016/j.cej.2012.02.041